

## Investigation of a Bubble Detector based on Active Electrolocation of Weakly Electric Fish

This content has been downloaded from IOPscience. Please scroll down to see the full text.

2013 J. Phys.: Conf. Ser. 434 012088

(<http://iopscience.iop.org/1742-6596/434/1/012088>)

View [the table of contents for this issue](#), or go to the [journal homepage](#) for more

### Download details:

IP Address: 134.94.122.242

This content was downloaded on 01/07/2015 at 12:24

Please note that [terms and conditions apply](#).

# Investigation of a Bubble Detector based on Active Electrolocation of Weakly Electric Fish

M Mohan<sup>1</sup>, K Mayekar<sup>2</sup>, R Zhou<sup>1</sup>, G von der Emde<sup>2</sup> and H Bousack<sup>1,\*</sup>

<sup>1</sup> Forschungszentrum Jülich, Peter Grünberg Institute PGI-8, Jülich, Germany

<sup>2</sup> University of Bonn, Institute of Zoology, Bonn, Germany

E-mail: \* h.bousack@fz-juelich.de

**Abstract.** Weakly electric fish employ active electrolocation for navigation and object detection. They emit an electric signal with their electric organ in the tail and sense the electric field with electroreceptors that are distributed over their skin. We adopted this principle to design a bubble detector that can detect gas bubbles in a fluid or, in principle, objects with different electric conductivity than the surrounding fluid. The evaluation of the influence of electrode diameter on detecting a given bubble size showed that the signal increases with electrode diameter. Therefore it appears that this detector will be more appropriate for large sized applications such as bubble columns than small sized applications such as bubble detectors in dialysis.

## 1. Introduction

The detection of gas bubbles in fluids is an important issue in areas such as medical technology or process engineering, for example during dialysis, infusions or two-phase flows. For these purposes, different measuring principles are used such as ultrasound, along with capacitive, thermal, optical or impedance sensors.

The sensor presented here is partly based on the principle of active electrolocation in the weakly electric fish, *Gnathonemus petersii*, and a simplified process tomography. Weakly electric fish orient in their environment and locate prey by means of an electrical field emitted from their tail as an electrical organ discharge. Objects with electrical properties other than those of the surrounding water distort the generated field. The fish perceives these distortions using about 3000 electroreceptor organs distributed over a large area of the its skin. Thus, an object within the range of the electrical field projects an electrical image onto the skin and the fish can determine object parameters, such as material, size, shape and distance [1]. Electrical impedance tomography (EIT) [2] uses a circular array of evenly spaced electrodes in a single plane of a vessel or several planes axially arranged. A pair of electrodes is connected with a sinusoidal current source and the resulting potential difference is measured between all electrode pairs. For the determination of the spatial distribution of the electrical conductivity above the plane surface based on the measured potential differences, an inverse problem must be solved. Hence, both *Gnathonemus petersii* and EIT use the spatial distribution of the electrical conductivity as an electrical image to detect and characterize objects.

## 2. Principle of the bubble detector

The method presented here uses two ring shaped electrodes arranged axially in a tube, see Fig. 1. Between the sending electrode (1 V, 1 KHz) and the receiving electrode an electrical field is

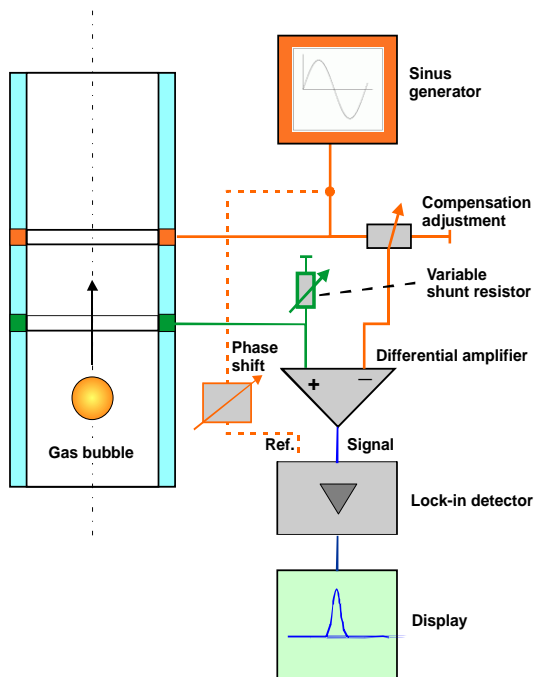


**Figure 1.** Principle of the measurements.

changes that influence the conductivity of the fluid. In addition, peaks due to high frequency interference can occur. For the removal of a low frequency drift, the airPLS function in MATLAB was used as a baseline correction. The signal was further smoothed by using a 2<sup>nd</sup> order Butterworth low pass filter with a cutoff frequency of 0.17 Hz before the peak analysis of the signals was carried out. The filtered time series is shown in the lower diagram in figure 2. Based on the filtered time series, a histogram and a best-fitting normal distribution was calculated, which allows assigning a mean and a standard deviation for each measurement. Using this procedure, all electrode sets were measured and evaluated.

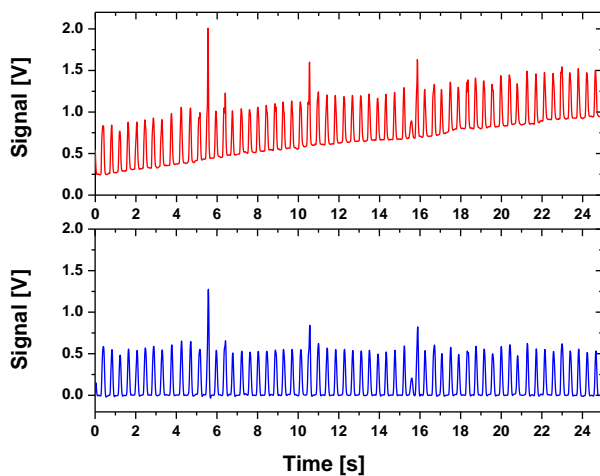


**Figure 2.** Time series of a bubble measurement. Above: raw data, below: filtered data. Parameters of the measurement: electrode diameter: 18 mm, electrode distance: 18 mm, air bubble diameter: 1mm, conductivity water: 80  $\mu$  S/cm.

generated, which is disturbed when an object, e.g. a gas bubble, passes through the rings. Similar to the fish and in contrast to EIT, the potential difference measured at the receiving electrode is processed by a differential amplifier that eliminates the signal sent. A lock-in detector, used as a narrowband amplifier tuned to the sending frequency, extracts the signal from the noisy environment [3]. Thus, a time-dependent signal of the object is received, averaged over the cross section of the tube.

### 3. Experiments

For an easy modification of the electrode diameter and distance, the electrodes were manufactured from silver plated wires with a diameter of 0.7 mm. Both wire electrodes were attached to a holder that allows an adjustment of the electrode distance. To ensure a geometrical similarity in all electrode sets, the distance between the electrodes was kept equal to the electrode diameter. Based on this, electrode sets with diameters of 14, 18, 26 and 33 mm were used in the experiments. The upper curve in figure 2 shows a time series measurement of bubbles with an increasing baseline. This increase is due to ambient temperature

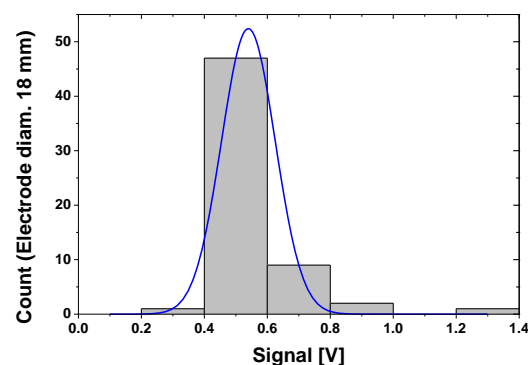


**Figure 3.** Histogram with superimposed best-fitting normal distribution for the time series shown in Fig. 2. The mean is 0.57 V, the median is 0.55 V and the standard deviation is 0.12 V. The diameter of the electrode is 18 mm and the diameter of the air bubble is 1 mm. Parameters of the measurement see Figure 2.

For control of reproducibility, the measurements were repeated several times on different days. It turned out that the reproducibility was not as good as expected. Several reasons are responsible for this: a) In general, the formation of a gas bubble detaching from a nozzle in a liquid is not stable, because the bubble surface tends to vibrate, and sometimes the bubble splits in two parts. b) During its rise, the bubble is flattening and spirals upward inducing turbulent water flow for the following bubbles. c) Due to the spiral path of the bubble and an unevenness of the electrical field as function of electrode radius, even two absolutely similar bubbles will generate slightly different signals. d) The mechanical stability of the fragile wire electrodes is insufficient, and the assembly of the same electrode set-up will result in a little different performance. The reasons a) to c) are system-inherent. Because of the real bubble behavior, different signals must be expected. Only the reason d) can be reduced by using more stable electrodes.

The reason a) was investigated with respect to the bubble formation. The tubing pump used (ISMATEC Reglo Digital MS-4/8, IDEX Health & Science, Oak Harbor, USA) allows to produce a continuous stream of bubbles or a single bubble on demand, which may result in more homogenous bubbles. Figure 4 shows a comparison of the mean of the bubble signal with standard deviation as a function of the different electrode sets using the continuous bubble flow and a series of single bubbles. Except for the electrode diameter of 33 mm, the signals of the different measurements are more or less the same, although the differences of the standard deviations of the two measurements with continuous bubble flows are remarkable. Here, the series of single bubbles appears to yield smaller deviations. A phase shift adjustment (see Fig. 1) can compensate the phase shift between the receiving and the sending electrode. For this reason, the phase shift adjustment influences the measured signal quality. In fig. 5, the influence of the phase shift is shown using a linear fit with the standard deviation as weight. Obviously, the consideration of the phase shift resulted in reduced signals and in a significantly lower standard deviation.

In summary, it can be concluded that the signal of the bubble detector increases almost linearly with the electrode diameter. This result is surprising because during the experiments, the bubble size stayed constant for the different electrode diameters, which lead to a decreasing relationship of the bubble cross section and the electrode cross section. Due to the larger field distortions, smaller electrode diameters should yield larger signals.

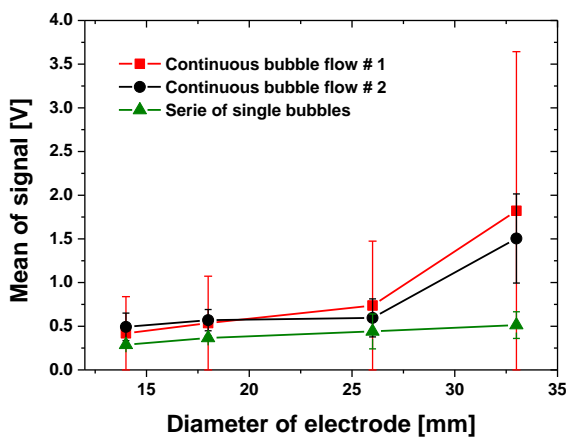


**Figure 4.** Comparison of the mean signals of continuous bubble flow and a series of single bubbles as function of the electrode diameter. The standard deviation is indicated. Parameters of the measurement: air bubble diameter: 1mm, conductivity water: 80  $\mu$  S/cm, phase shift  $\varphi = 0^\circ$

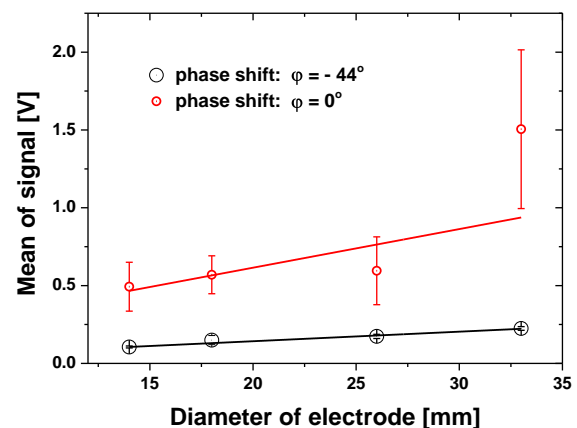


**Figure 5.** Comparison of the mean signals of continuous bubble flow with different phase shift. The standard deviation is indicated. Parameters of the measurement: see Fig. 4.

#### 4. Simulation

For the purpose of securing the principal linear course of the signal as a function of the electrode diameter, a finite element (FEM) analysis was carried out. Figure 6 shows the calculated field distribution of the electric potential with and without a bubble. It is obvious that for lower distances of the electrodes, the radial field distribution is inhomogeneous, which causes different signals depending on the radial position of the bubble. Furthermore it is evident that the field deformation is very small. Using this model, the diameters of the electrodes were varied between 15 mm and 40 mm, while all other parameters stayed constant. In figure 7, the calculation of the current in the shunt resistor (Fig. 1) resulted in a linear dependence of the current from the diameter of the electrodes. This confirmed the experimental result, which suggested a linear dependence.

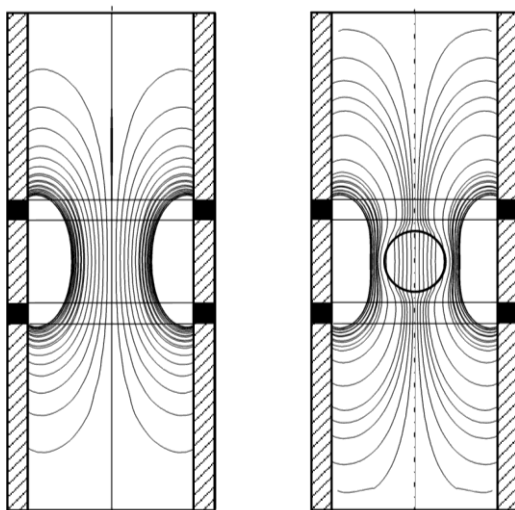


**Figure 6.** Field distribution of the electric potential without air bubble (left) and with air bubble (right). Parameters see Fig. 7

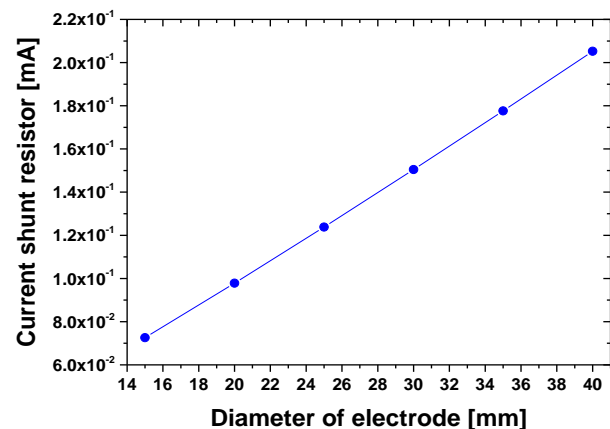


**Figure 7.** Simulation of the current in the shunt resistor as function of the electrode diameter. Parameters are: distance electrodes 10 mm, conductivity water 5  $\mu\text{S}/\text{cm}$ , air bubble diameter 10 mm

#### References

- [1] von der Emde G *et al* 2010 3-Dimensional Scene Perception during Active Electrolocation in a Weakly Electric Pulse Fish *Frontiers in behavioral neuroscience* **4** 26
- [2] York T 2001 Status of electrical tomography in industrial applications *J Electron Imaging* **10** 608
- [3] Bousack H *et al* 2012 patent application Blasendetektor Forschungszentrum Jülich and Universität Bonn